PHYSICAL REVIEW B **111**, L140409 (2025)

Letter | Editors' Suggestion

Orbital pumping by magnetization dynamics in ferromagnets

Dongwook Go,[1,2,*] Kazuya Ando,[3,4,5] Armando Pezo,[6] Stefan Blügel,[1] Aurélien Manchon,[7] and Yuriy Mokrousov[1,2]

[1]*Peter Grünberg Institut, Forschungszentrum Jülich, 52425 Jülich, Germany*
[2]*Institute of Physics, Johannes Gutenberg University Mainz, 55099 Mainz, Germany*
[3]*Department of Applied Physics and Physico-Informatics, Keio University, Yokohama 223-8522, Japan*
[4]*Keio Institute of Pure and Applied Sciences (KiPAS), Keio University, Yokohama 223-8522, Japan*
[5]*Center for Spintronics Research Network (CSRN), Keio University, Yokohama 223-8522, Japan*
[6]*Laboratoire Albert Fert, CNRS, Thales, Université Paris-Saclay, Palaiseau 91767, France*
[7]*Aix-Marseille Université, CNRS, CINaM, Marseille, France*

(Received 9 March 2024; revised 21 May 2024; accepted 18 March 2025; published 16 April 2025)

We show that dynamics of the magnetization in ferromagnets can pump orbital angular momentum, a phenomenon we refer to as orbital pumping. This is the reciprocal phenomenon to orbital torque that induces magnetization dynamics by the orbital angular momentum in nonequilibrium. The orbital pumping is analogous to the spin pumping established in spintronics, but it requires spin-orbit coupling for the orbital angular momentum to interact with magnetization. We develop a formalism that describes the generation of orbital angular momentum by magnetization dynamics within the adiabatic perturbation theory. Based on this, we perform first-principles calculations of orbital pumping in prototypical 3*d* ferromagnets, Fe, Co, and Ni. Results show that the ratio between orbital pumping and spin pumping ranges from 5% to 15%, being smallest in Fe and largest in Ni. This implies that ferromagnetic Ni is a good candidate for measuring the orbital pumping. Implications of our results on experiments are also discussed.

DOI: 10.1103/PhysRevB.111.L140409

Injection of spin into a ferromagnet (FM) can induce magnetization dynamics, which is called spin torque [1–5]. The reciprocal effect known as spin pumping can generate nonequilibrium spin by magnetization dynamics [6–10]. The spin torque and pumping have played pivotal roles in spintronics as means of manipulating the magnetization and generating spin currents, respectively [11,12]. In general, however, the physical mechanism of magnetization dynamics is governed by transfer of the *angular momentum* [13,14], which is not restricted to the spin. As a result, a recent theory has shown that nonequilibrium orbital angular momentum (OAM) can also induce magnetization dynamics [15], which is denoted by orbital torque. A crucial difference between the spin torque and the orbital torque is that the orbital torque requires spin-orbit coupling (SOC) because local moments in a ferromagnet are coupled to spin by the exchange interaction, and the OAM interacts with magnetization *indirectly* via SOC. Thus, the orbital torque depends sensitively on the way the spin and orbital characters are entangled for the states near the Fermi energy [14,16]. The orbital torque has been measured in several experiments in recent years, via the sign change, crucial dependence on the choice of a ferromagnet, and orbital-to-spin conversion [16–24].

A natural question that arises is what are the properties of the reciprocal phenomenon to the orbital torque. We may refer to this effect by *orbital pumping*, the generation of nonequilibrium OAM from magnetization dynamics, whose concept is schematically illustrated in Fig. 1. Recently, Hayashi *et al.* reported an experimental observation of the orbital pumping in Ti/Ni bilayers [25]. Here, ferromagnetic resonance generates OAM together with spin in Ni, which is injected across the interface. The injected OAM in Ti is electrically measured by using the inverse orbital Hall effect, where the inverse spin Hall effect is negligibly small due to small SOC [26–28]. This result is consistent with the recent observation of large orbital Hall effect in Ti [27] and orbital torque measurement that finds pronounced torque response when Ni is used as a ferromagnet [23]. Interestingly, Hayashi *et al.* found that the signal is significantly suppressed in Ti/Fe bilayers [25], implying that the orbital pumping is less pronounced in Fe. One may ask why orbital pumping differs in Fe and Ni. This motivates us to investigate its microscopic origin and perform quantitative evaluation of the orbital pumping in 3*d* ferromagnets.

In this Letter, we develop a formalism describing the orbital pumping within the adiabatic perturbation theory and derive a Green's function expression for the generation of the OAM by magnetization dynamics. From first principles, we compute the orbital pumping in ferromagnetic Fe, Co, and Ni. We show that the orbital pumping is a concomitant effect of the spin pumping due to the SOC and thus exhibits a Hund-rule-like behavior [29,30], evolving from the negative

*Contact author: d.go@fz-juelich.de

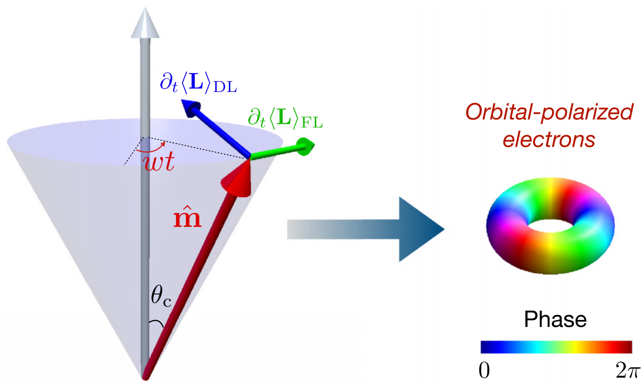

FIG. 1. In the presence of the SOC in a FM, magnetization dynamics induces nonequilibrium OAM of electrons, which we denote by orbital pumping. The donut schematically shows $|l=2,m=2\rangle = (|x^2-y^2\rangle + i|xy\rangle)/\sqrt{2}$ wave function, where the color represents the complex phase.

to the positive value as the occupation number of the d shell increases. The magnitude of the orbital pumping ranges from 5% to 15% of that of the spin pumping in Fe, Co, and Ni, being smallest in Fe and largest in Ni. This result is in agreement with the recent experiment measuring significant orbital pumping contribution in Ti/Ni [25], but nearly complete suppression of the signal in Ti/Fe and Ti/Co cannot be explained by the bulk property of Fe alone.

We define the orbital pumping as the response of $\partial_t\langle\mathbf{L}\rangle$ to the magnetization dynamics, where $\mathbf{L}$ is the OAM operator. This can be formally written as a linear response expression,

$$\partial_t\langle L_\alpha\rangle = \sum_\beta \chi^L_{\alpha\beta}(\hat{\mathbf{m}}\times\partial_t\hat{\mathbf{m}})_\beta, \tag{1}$$

where $\hat{\mathbf{m}}$ is the unit vector of the magnetization, and α,β are Cartesian indices. Note that $\hat{\mathbf{m}}\times\partial_t\hat{\mathbf{m}}$ acts as a generalized force, pointing in the direction of Gilbert damping. As shown in Fig. 1, $\partial_t\langle\mathbf{L}\rangle$ can be conveniently decomposed into fieldlike and dampinglike components, which point in the directions of $\partial_t\hat{\mathbf{m}}$ and $\hat{\mathbf{m}}\times\partial_t\hat{\mathbf{m}}$, respectively. Let us consider a situation of the magnetization precessing around a certain axis (grey arrow) with the cone angle θ_c and angular frequency w. For convenience, let us define Cartesian coordinates such that x, y, and z are axes parallel to $\partial_t\hat{\mathbf{m}}$, $\hat{\mathbf{m}}\times\partial_t\hat{\mathbf{m}}$, and $\hat{\mathbf{m}}$, respectively. From Eq. (1), we find $\partial_t\langle\mathbf{L}\rangle_{\rm FL} = \hat{\mathbf{x}}\chi^L_{xy}w\sin\theta_c$ and $\partial_t\langle\mathbf{L}\rangle_{\rm DL} = \hat{\mathbf{y}}\chi^L_{yy}w\sin\theta_c$, where $w\sin\theta_c$ is the norm of $\hat{\mathbf{m}}\times\partial_t\hat{\mathbf{m}}$. Both the fieldlike and dampinglike components have AC responses, but the projection of the dampinglike component on the precession axis generates a DC response, which is given by $\chi^L_{yy}w\sin^2\theta_c$. We emphasize that assuming that θ_c is small enough, which is the case for prototypical $3d$ ferromagnets [31–33] ($\theta_c \lesssim 1-10^\circ$), $\chi^L_{\alpha\beta}$ may be computed for a fixed configuration of $\hat{\mathbf{m}}$ along an easy axis. Experimentally, θ_c can be obtained by the microwave photoresistance measurement [34]. Meanwhile, when the electronic structure undergoes significant changes due to variations in $\hat{\mathbf{m}}$, the orbital pumping coefficient can be calculated along the trajectory of $\hat{\mathbf{m}}$ and integrated over the cycle, in a manner similar to the theory of adiabatic charge pumping [35–37].

To evaluate $\chi^L_{\alpha\beta}$ from the electronic structure, we apply the adiabatic perturbation theory [38], in which $\hat{\mathbf{m}}$ evolves slowly enough for the electronic eigenstates to evolve adiabatically without making transitions. Note that the magnetization dynamics in GHz range, which corresponds to 10^{-6} eV, is sufficiently slower than the dynamics of electrons. From this, we derive a Green's function's expression for $\chi^L_{\alpha\beta}$ (see the Supplemental Material [39]) in the Bastin-Smrčka-Středa form [40–42] of the Kubo formula [43],

$$\chi^L_{\alpha\beta,\rm even} = \frac{\hbar}{4\pi}\int d\mathcal{E}\,(\partial_\mathcal{E} f) \times \mathrm{Tr}\big[T^{L_\alpha}_{\rm tot}(G^{\rm R}-G^{\rm A})T^{S_\beta}_{\rm XC}(G^{\rm R}-G^{\rm A})\big], \tag{2a}$$

$$\chi^L_{\alpha\beta,\rm odd} = \frac{\hbar}{4\pi}\int d\mathcal{E} f \times \mathrm{Tr}\big[T^{L_\alpha}_{\rm tot}(G^{\rm R}-G^{\rm A})T^{S_\beta}_{\rm XC}(\partial_\mathcal{E}G^{\rm R}+\partial_\mathcal{E}G^{\rm A}) - T^{L_\alpha}_{\rm tot}(\partial_\mathcal{E}G^{\rm R}+\partial_\mathcal{E}G^{\rm A})T^{S_\beta}_{\rm XC}(G^{\rm R}-G^{\rm A})\big], \tag{2b}$$

where $G^{\rm R/A} = 1/(\mathcal{E}-\mathcal{H}_{\rm tot}\pm i\Gamma)$ is the retarded/advanced Green's function, $\mathcal{H}_{\rm tot}$ is the total Hamiltonian, and $\mathcal{E}$ is the energy. The energy broadening Γ effectively describes the relaxation of the electron quasiparticles by scatterings. The Fermi-Dirac distribution function f is defined at energy $\mathcal{E}$. The operators $T^{L_\alpha}_{\rm tot} = [L_\alpha,\mathcal{H}_{\rm tot}]/i\hbar$ and $T^{S_\beta}_{\rm XC} = [S_\beta,\mathcal{H}_{\rm XC}]/i\hbar = J(\mathbf{r})\hat{\mathbf{m}}\times\mathbf{S}$ are the total torque on the α component of the OAM and the *exchange* torque on the β component of the spin, respectively. Here, $\mathcal{H}_{\rm XC} = J(\mathbf{r})\,\hat{\mathbf{m}}\cdot\mathbf{S}$ is the exchange potential. In Eq. (2), we adopt the decomposition depending on the time-reversal parity of the response [44]. Meanwhile, the analogous expression of Eq. (1) for the spin pumping can be obtained by replacing L_α by S_α in Eq. (2), which agrees with the expression derived in Refs. [45,46].

On the other hand, the linear response expression for the orbital torque is given by

$$\langle T^{S_\alpha}_{\rm XC}\rangle = \sum_\beta \tilde{\chi}^L_{\alpha\beta}B^L_\beta, \tag{3}$$

where B^L_β is an effective field that couples to the OAM by the Zeeman interaction $\mathcal{H}_L = \mathbf{B}_L\cdot\mathbf{L}$. It effectively describes a situation where non-equilibrium OAM is induced, for example, by orbital Hall effect [47–49] or orbital Edelstein effect [50–52]. Note that both $\partial_t\langle\mathcal{H}_L\rangle = \partial_t\langle\mathbf{L}\rangle\cdot\mathbf{B}^L$ and $\partial_t\langle\mathcal{H}_{\rm XC}\rangle = \langle T^{\mathbf{S}}_{\rm XC}\rangle\cdot(\hat{\mathbf{m}}\times\partial_t\hat{\mathbf{m}}) = \langle J\mathbf{S}\rangle\cdot\partial_t\hat{\mathbf{m}}$ have the unit of *power*. The expression for $\tilde{\chi}^L_{\beta\alpha}$ can also be derived similarly to Eq. (2), by which the reciprocal relation

$$\chi^L_{\alpha\beta} = \tilde{\chi}^L_{\beta\alpha} \tag{4}$$

can be explicitly shown [39]. We quantitatively evaluate the spin pumping and orbital pumping in prototypical $3d$ ferromagnets: bcc Fe, hcp Co, and fcc Ni. We set the magnetization $\hat{\mathbf{m}} = -\hat{\mathbf{z}}$. Details of the computational method can be found in the Supplemental Material [39]. For all Fe, Co, and Ni, only $\chi^L_{xx,\rm even}$ and $\chi^L_{yy,\rm even}$ are nonzero for the $\mathcal{T}$-even part [Eq. (2a)], and only $\chi^L_{xy,\rm odd}$ and $\chi^L_{yx,\rm odd}$ are nonzero for the $\mathcal{T}$-odd part [Eq. (2b)], where $\mathcal{T}$ is the time reversal. This constraint comes from the $\mathcal{TM}$ symmetry of the systems,

TABLE I. The ratio between the orbital pumping and spin pumping in Fe, Co, and Ni for the diagonal and off-diagonal responses, obtained for $\Gamma = 25$ and 100 meV of the energy broadening.

Material	χ^L_{xx}/χ^S_{xx} (%)	χ^L_{xy}/χ^S_{xy} (%)
Fe (25 meV)	6.08	4.38
Co (25 meV)	9.87	9.62
Ni (25 meV)	11.08	15.10
Fe (100 meV)	7.19	4.39
Co (100 meV)	9.53	9.32
Ni (100 meV)	10.64	14.12

where $\mathcal{M}$ is the reflection with respect to a mirror plane containing the magnetization [39]. Therefore, we drop "even" and "odd" in the subscript of $\chi^L_{\alpha\beta}$ and $\chi^S_{\alpha\beta}$ in the discussion below. We remark that the diagonal and off-diagonal components of the response tensor correspond to dampinglike and fieldlike torques, respectively.

The results for the ratios χ^L_{xx}/χ^S_{xx} and χ^L_{xy}/χ^S_{xy} are summarized in Table I. The ratios are between 5% and 15%, and the magnitudes are in the order of Fe < Co < Ni. We find that the ratios are nearly the same for the two chosen values of the energy broadening Γ, 25 and 100 meV, implying that the relative magnitude between the orbital pumping and spin pumping is robust with respect to the degree of disorder. In order to understand what makes Fe, Co, and Ni different, we investigate Fermi energy dependence of both diagonal (χ^S_{xx} and χ^L_{xx}) and off-diagonal (χ^S_{xy} and χ^L_{xy}) components of the response, which are shown in Figs. 2(a), 2(b) and Figs. 2(c), 2(d), respectively. The sign for the spin pumping [Figs. 2(a) and 2(c)] remains positive over a wide range of energy because the spin pumping is mainly due to the exchange spin splitting. The orbital pumping, however, exhibits gradual change of the sign, from negative to positive values [Figs. 2(b) and 2(d)]. We confirm that the orbital pumping is linearly proportional to the SOC strength and vanishes if SOC is switched off [39]. That is, the orbital pumping is a secondary effect following the spin pumping by the SOC. This also explains the small magnitude of the orbital pumping [Figs. 2(b) and 2(d)] compared to the the spin pumping [Figs. 2(a) and 2(c)] by an order of magnitude.

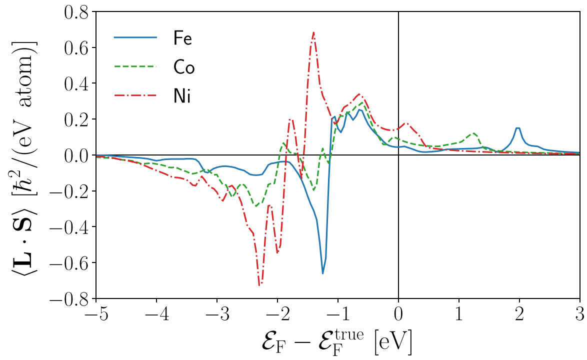

FIG. 3. Correlation between **L** and **S** at the Fermi surface.

For transition metals, Hund's third rule [29,30] states that when the d shell is approximately less than half-filled, the correlation between **L** and **S** is negative, $\langle \mathbf{L}\cdot\mathbf{S}\rangle < 0$, thus the spin pumping and orbital pumping exhibit the opposite signs. When the d shell is more than half-filled, the correlation becomes positive $\langle \mathbf{L}\cdot\mathbf{S}\rangle > 0$, thus the spin pumping and orbital pumping have the same sign. The correlations between **L** and **S** for the states at the Fermi surface in Fe, Co, and Ni are shown in Fig. 3. In all Fe, Co, and Ni, $\langle \mathbf{L}\cdot\mathbf{S}\rangle$ evolve

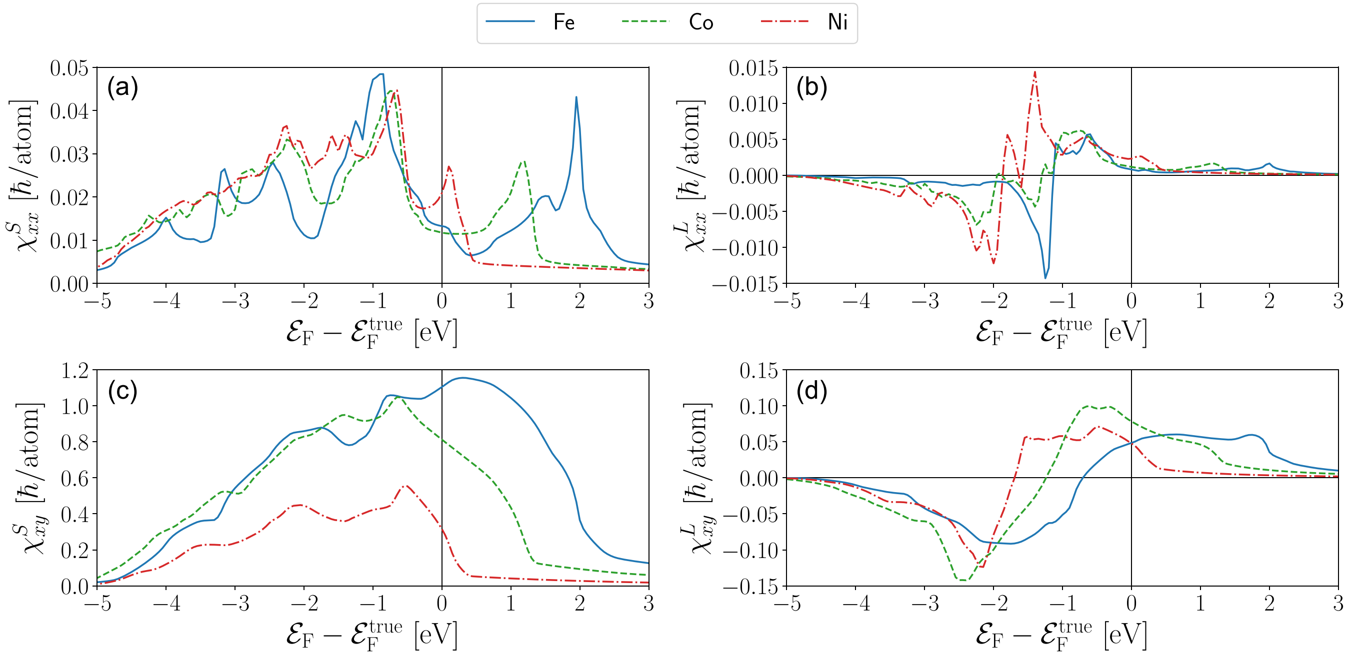

FIG. 2. The plots of the Fermi energy ($\mathcal{E}_\mathrm{F}$) dependence of (a) χ^S_{xx} and (b) χ^L_{xx}, for the spin pumping and orbital pumping, respectively. The same plots for χ^S_{xy} and χ^L_{xy} are shown in (c) and (d), respectively. The energy broadening is set to $\Gamma = 25$ meV in evaluating Eq. (2). The Fermi energy is varied with respect to the true value $\mathcal{E}_\mathrm{F}^\mathrm{true}$ within the rigid band approximation.

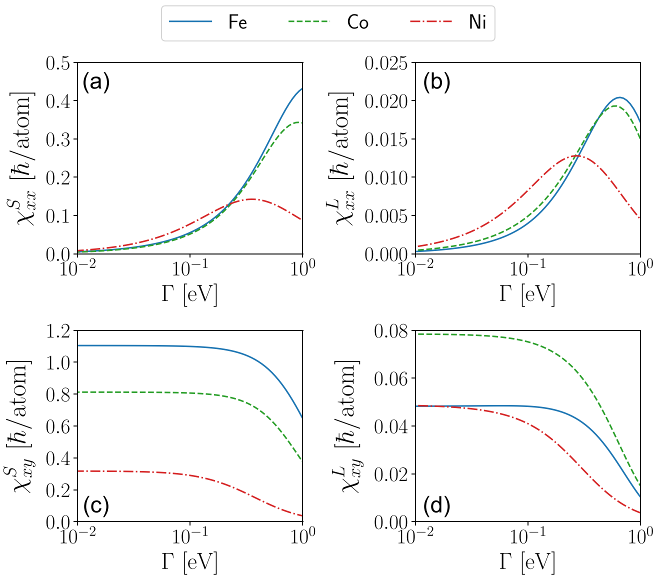

FIG. 4. The plots of the energy broadening (Γ) dependence of (a) χ^S_{xx} and (b) χ^L_{xx}, for the spin pumping and orbital pumping, respectively. The same plots for χ^S_{xy} and χ^L_{xy} are shown in (c) and (d), respectively.

from negative values to positive values as the Fermi energy gradually increases. Note the stark resemblance between Figs. 2(b) and 3, which clearly demonstrates the crucial role of the correlation between the orbital and spin angular momenta in the orbital pumping.

In general, we find that the diagonal component [Figs. 2(a) and 2(b)] exhibits more rapid variation as a function of the energy, as compared to the off-diagonal component [Figs. 2(c) and 2(d)]. This is because the $\mathcal{T}$-even [Eq. (2a)] and $\mathcal{T}$-odd responses [Eq. (2b)] capture the contributions at the Fermi *surface* and from the Fermi *sea*, respectively. At zero temperature, Eq. (2a) becomes

$$\chi^L_{\alpha\beta,\mathrm{even}} = \frac{\hbar}{\pi}\sum_{\mathbf{k}}\sum_{nm} A_{n\mathbf{k}}(\mathcal{E}_\mathrm{F})A_{m\mathbf{k}}(\mathcal{E}_\mathrm{F}) \times \mathrm{Re}\big[\langle\psi_{n\mathbf{k}}|T^{L_\alpha}_{\mathrm{tot}}|\psi_{m\mathbf{k}}\rangle\langle\psi_{m\mathbf{k}}|T^{S_\beta}_{\mathrm{XC}}|\psi_{n\mathbf{k}}\rangle\big], \quad (5)$$

where $\psi_{n\mathbf{k}}$ is the Bloch state with band index n and crystal momentum $\mathbf{k}$, and $A_{n\mathbf{k}}(\mathcal{E}_\mathrm{F}) = \Gamma/[(\mathcal{E}_\mathrm{F}-\mathcal{E}_{n\mathbf{k}})^2+\Gamma^2]$ is the spectral function at the Fermi energy, and $\mathcal{E}_{n\mathbf{k}}$ is the energy dispersion. On the other hand, the $\mathcal{T}$-odd response [Eq. (2b)] has an *intrinsic limit* even in the zeroth order of Γ,

$$\chi^L_{\alpha\beta,\mathrm{odd}} \approx \hbar\sum_{\mathbf{k}}\sum_{n\neq m}(f_{n\mathbf{k}}-f_{m\mathbf{k}}) \times \frac{\mathrm{Im}\big[\langle\psi_{n\mathbf{k}}|T^{L_\alpha}_{\mathrm{tot}}|\psi_{m\mathbf{k}}\rangle\langle\psi_{m\mathbf{k}}|T^{S_\beta}_{\mathrm{XC}}|\psi_{n\mathbf{k}}\rangle\big]}{(\mathcal{E}_{n\mathbf{k}}-\mathcal{E}_{m\mathbf{k}})^2}, \quad (6)$$

where $f_{n\mathbf{k}}$ is the Fermi-Dirac distribution function.

Because of this, the diagonal and off-diagonal responses exhibit different behaviors as a function of the energy broadening Γ. Figures 4(a) and 4(b) show the Γ dependence of χ^S_{xx} and χ^L_{xx}, respectively. Interestingly, both of them exhibit nonmonotonic behavior. They tend to increase from the ultraclean regime ($\Gamma \approx 0$) to the moderately clean regime ($\Gamma \sim 10^{-1}$ eV), but as Γ further increases toward a disordered regime ($\Gamma \sim 1$ eV) the magnitudes start to decrease. This suggests that samples need to be moderately clean but not too clean to have sizable magnitude of χ^S_{xx} and χ^L_{xx}. We emphasize that expressions like Eq. (5) often exhibit a conductivity-like $\propto 1/\Gamma$ behavior because the band-diagonal term ($n = m$) is proportional to $A_{n\mathbf{k}}(\mathcal{E}_\mathrm{F})A_{n\mathbf{k}}(\mathcal{E}_\mathrm{F}) \approx (\pi/\Gamma)\delta(\mathcal{E}_\mathrm{F}-\mathcal{E}_{n\mathbf{k}})$ in the small Γ limit [44,53]. However, χ^S_{xx} and χ^L_{xx} show a quadratic $\propto \Gamma^2$ behavior because the band-diagonal component of the torque-torque correlation in Eq. (5) is absent. Therefore, spectral mixing of bands at the Fermi energy is crucial for χ^S_{xx} and χ^L_{xx}. We note that nonmonotonic dependence on the broadening has been found in the study of Gilbert damping [54,55].

On the other hand, χ^S_{xy} and χ^L_{xy} shown in Figs. 4(c) and 4(d), respectively, are stable up to moderate strength of the broadening, displaying a typical intrinsic behavior. In general, we find that the spin pumping [Figs. 4(a) and 4(c)] is more robust with respect to Γ when compared to the orbital pumping [Figs. 4(b) and 4(d)]. This is because the relevant energy scale of the spin pumping is the exchange interaction, which is of the order of ∼1 eV. In contrast, the SOC is necessary for the orbital pumping, whose energy scale is an order of magnitude smaller than the exchange interaction.

The experimental work by Hayashi *et al.* measured the DC component of the orbital pumping [25], which corresponds to $\chi^L_{xx} w \sin^2\theta_\mathrm{c}$ in our theory. They found that the orbital pumping is significant in Ti/Ni while the effect is nearly absent in Ti/Fe, which seems consistent with our theoretical calculation. However, the numerical value of χ^L_{xx} for Ni is approximately three times larger than that for Fe, which cannot explain almost complete suppression of the signal in Ti/Fe and Ti/Co samples. Therefore, we conclude that the orbital pumping in the bulk ferromagnet alone cannot explain the experimental result. We speculate that the OAM transmission or transparency at the interfaces of Ti/Fe and Ti/Co could be much lower than that at the Ti/Ni interface. Meanwhile, another experimental work [56] reports substantial amplitude of the orbital pumping in Ti/Co.

Recent terahertz spectroscopy experiments have revealed that ferromagnetic Ni can generate the OAM by laser excitation [57–59]. Although the dynamics of magnetic moments is incoherent, which is different from the ferromagnetic resonance, we remark that the DC component projected onto the precession axis does not cancel as it is phase -independent (Fig. 1). Thus, our results imply that excitation of incoherent magnons by laser or temperature can induce OAM. In particular, we predict that when the gradient of such excitation is present, so-called *orbital Seebeck effect* may appear by a mechanism similar to orbital pumping. Recently, El Hamdi *et al.* showed that a temperature gradient can generate orbital currents, which is electrically measured via the inverse orbital Edelstein effect [60]. The experiment suggests that 6% of the OAM is injected compared to the spin for ferromagnetic Permalloy, which is in reasonable agreement with our calculation (Table I). In ferromagnets with low crystal symmetry, another mechanism that induces OAM from the thermal fluctuations of magnetic moments is via magnon-mediated chirality [61], which can result in an anomalous behavior of the g factor as a function of the temperature [62]. The OAM can also be generated by combining the spin pumping and the spin-to-orbital conversion, which can be achieved by adding an insertion layer with strong SOC such as Pt [63,64]. This could be a promising route to enhancing the orbital pumping by overcoming the limitation due to the weak SOC of the FM.

Spin pumping is known to enhance Gilbert damping due to loss of angular momentum from the magnetization to electrons [6,7], which has been demonstrated in experiments [65,66] as well as by first-principles calculations [67]. Analogously, the orbital pumping is generally expected to increase Gilbert damping as OAM is transferred from the magnetization to electrons, considering the conservation of the total angular momentum. However, as we have shown by our first-principles calculations (Fig. 2 and Table I), orbital pumping is an order of magnitude smaller than spin pumping. This implies that the orbital pumping contribution to the damping enhancement would be smaller than the spin pumping contribution. This is consistent with the experiment by Hayashi *et al.*, which found that the variation of Gilbert damping is not appreciable in Ti/Ni bilayers [25].

Previously, the theory of spin pumping was developed within the magnetoelectric circuit theory [6,7], which relies on the boundary condition together with the conservation of the total spin. However, its generalization to the orbital pumping is far from straightforward, because the conservation of the OAM is strongly violated due to its coupling to the lattice [14,68]. Note that Ref. [69] obtained result analogous to the spin pumping theory in the limit where the OAM is conserved. Meanwhile, first-principles calculations of the orbital pumping in prototypical magnetic bilayers can be found in Ref. [70], which qualitatively confirms our conclusions and discusses the role of orbital injection through the interface of transition metals.

In conclusion, we have developed a theoretical formalism that describes the orbital pumping in ferromagnets. Unlike the spin pumping, the orbital pumping crucially depends on the SOC. We have performed first-principles calculations on ferromagnetic Fe, Co, and Ni for quantitative estimation of the orbital pumping. The results shows that the orbital pumping is strongest in Ni and weakest in Fe, and its magnitude ranges from 5% to 15% compared to the magnitude of the spin pumping. Our work opens the possibility of generating the OAM by magnetization dynamics and serves as a guideline for experiments.

D.G. acknowledges stimulating discussion with Michel Viret, Cosimo Gorini, and Giovanni Vignale. This work was supported by the EIC Pathfinder OPEN Grant No. 101129641 "OBELIX." D.G. and Y.M. acknowledge the funding by the Deutsche Forschungsgemeinschaft TRR 173/3-268565370 (Project 629 No. A11) and TRR 288–422213477 (Project No. B06). K.A. acknowledges the support by JSPS KAKENHI (Grants No. 22H04964, No. 20H00337, and No. 20H02593), Spintronics Research Network of Japan (Spin-RNJ), and MEXT Initiative to Establish Next-generation Novel Integrated Circuits Centers (X-NICS) (Grant No. JPJ011438). A.P. acknowledges support from the ANR ORION Project, Grant No. ANR-20-CE30-0022-01 of the French Agence Nationale de la Recherche. A.M. acknowledges support from the Excellence Initiative of Aix-Marseille Université–A*Midex, a French "Investissements d'Avenir" program. We also gratefully acknowledge the Jülich Supercomputing Centre and RWTH Aachen University for providing computational resources under Projects cjiff40 and jara0062.

[1] J. C. Slonczewski, Current-driven excitation of magnetic multilayers, J. Magn. Magn. Mater. **159**, L1 (1996).
[2] L. Berger, Emission of spin waves by a magnetic multilayer traversed by a current, Phys. Rev. B **54**, 9353 (1996).
[3] E. B. Myers, D. C. Ralph, J. A. Katine, R. N. Louie, and R. A. Buhrman, Current-induced switching of domains in magnetic multilayer devices, Science **285**, 867 (1999).
[4] M. D. Stiles and A. Zangwill, Anatomy of spin-transfer torque, Phys. Rev. B **66**, 014407 (2002).
[5] D. C. Ralph and M. D. Stiles, Spin transfer torques, J. Magn. Magn. Mater. **320**, 1190 (2008).
[6] Y. Tserkovnyak, A. Brataas, and G. E. W. Bauer, Enhanced Gilbert damping in thin ferromagnetic films, Phys. Rev. Lett. **88**, 117601 (2002).
[7] Y. Tserkovnyak, A. Brataas, and G. E. W. Bauer, Spin pumping and magnetization dynamics in metallic multilayers, Phys. Rev. B **66**, 224403 (2002).
[8] S. Mizukami, Y. Ando, and T. Miyazaki, Effect of spin diffusion on Gilbert damping for a very thin permalloy layer in Cu/permalloy/Cu/Pt films, Phys. Rev. B **66**, 104413 (2002).
[9] A. Azevedo, L. H. Vilela Leão, R. L. Rodriguez-Suarez, A. B. Oliveira, and S. M. Rezende, dc effect in ferromagnetic resonance: Evidence of the spin-pumping effect? J. Appl. Phys. **97**, 10C715 (2005).
[10] E. Saitoh, M. Ueda, H. Miyajima, and G. Tatara, Conversion of spin current into charge current at room temperature: Inverse spin-Hall effect, Appl. Phys. Lett. **88**, 182509 (2006).
[11] Y. Tserkovnyak, A. Brataas, G. E. W. Bauer, and B. I. Halperin, Nonlocal magnetization dynamics in ferromagnetic heterostructures, Rev. Mod. Phys. **77**, 1375 (2005).
[12] A. Brataas, Y. Tserkovnyak, G. E. W. Bauer, and P. J. Kelly, Spin pumping and spin transfer, in *Spin Current* (Oxford University Press, Oxford, 2017).
[13] P. M. Haney and M. D. Stiles, Current-induced torques in the presence of spin-orbit coupling, Phys. Rev. Lett. **105**, 126602 (2010).
[14] D. Go, F. Freimuth, J.-P. Hanke, F. Xue, O. Gomonay, K.-J. Lee, S. Blügel, P. M. Haney, H.-W. Lee, and Y. Mokrousov, Theory of current-induced angular momentum transfer dynamics in spin-orbit coupled systems, Phys. Rev. Res. **2**, 033401 (2020).
[15] D. Go and H.-W. Lee, Orbital torque: Torque generation by orbital current injection, Phys. Rev. Res. **2**, 013177 (2020).
[16] D. Lee, D. Go, H.-J. Park, W. Jeong, H.-W. Ko, D. Yun, D. Jo, S. Lee, G. Go, J. H. Oh, K.-J. Kim, B.-G. Park, B.-C. Min, H. C. Koo, H.-W. Lee, O. Lee, and K.-J. Lee, Orbital torque in magnetic bilayers, Nat. Commun. **12**, 6710 (2021).
[17] S. Ding, A. Ross, D. Go, L. Baldrati, Z. Ren, F. Freimuth, S. Becker, F. Kammerbauer, J. Yang, G. Jakob, Y. Mokrousov, and

M. Kläui, Harnessing orbital-to-spin conversion of interfacial orbital currents for efficient spin-orbit torques, Phys. Rev. Lett. **125**, 177201 (2020).
[18] J. Kim, D. Go, H. Tsai, D. Jo, K. Kondou, H.-W. Lee, and Y. Otani, Nontrivial torque generation by orbital angular momentum injection in ferromagnetic-metal/Cu/Al_2O_3 trilayers, Phys. Rev. B **103**, L020407 (2021).
[19] S. Lee, M.-G. Kang, D. Go, D. Kim, J.-H. Kang, T. Lee, G.-H. Lee, J. Kang, N. J. Lee, Y. Mokrousov, S. Kim, K.-J. Kim, K.-J. Lee, and B.-G. Park, Efficient conversion of orbital Hall current to spin current for spin-orbit torque switching, Commun. Phys. **4**, 234 (2021).
[20] G. Sala and P. Gambardella, Giant orbital Hall effect and orbital-to-spin conversion in $3d$, $5d$, and $4f$ metallic heterostructures, Phys. Rev. Res. **4**, 033037 (2022).
[21] S. Dutta and A. A. Tulapurkar, Observation of nonlocal orbital transport and sign reversal of dampinglike torque in Nb/Ni and Ta/Ni bilayers, Phys. Rev. B **106**, 184406 (2022).
[22] L. Liao, F. Xue, L. Han, J. Kim, R. Zhang, L. Li, J. Liu, X. Kou, C. Song, F. Pan, and Y. Otani, Efficient orbital torque in polycrystalline ferromagnetic-metal/Ru/Al_2O_3 stacks: Theory and experiment, Phys. Rev. B **105**, 104434 (2022).
[23] H. Hayashi, D. Jo, D. Go, T. Gao, S. Haku, Y. Mokrousov, H.-W. Lee, and K. Ando, Observation of long-range orbital transport and giant orbital torque, Commun. Phys. **6**, 32 (2023).
[24] A. Bose, F. Kammerbauer, R. Gupta, D. Go, Y. Mokrousov, G. Jakob, and M. Kläui, Detection of long-range orbital-Hall torques, Phys. Rev. B **107**, 134423 (2023).
[25] H. Hayashi, D. Go, S. Haku, Y. Mokrousov, and K. Ando, Observation of orbital pumping, Nat. Electron. **7**, 646 (2024).
[26] L. Salemi and P. M. Oppeneer, First-principles theory of intrinsic spin and orbital Hall and Nernst effects in metallic monoatomic crystals, Phys. Rev. Mater. **6**, 095001 (2022).
[27] Y.-G. Choi, D. Jo, K.-H. Ko, D. Go, K.-H. Kim, H. G. Park, C. Kim, B.-C. Min, G.-M. Choi, and H.-W. Lee, Observation of the orbital Hall effect in a light metal Ti, Nature (London) **619**, 52 (2023).
[28] D. Go, H.-W. Lee, P. M. Oppeneer, S. Blügel, and Y. Mokrousov, First-principles calculation of orbital Hall effect by Wannier interpolation: Role of orbital dependence of the anomalous position, Phys. Rev. B **109**, 174435 (2024).
[29] F. Hund, On the interpretation of intricate spectra, in particular the elements scandium to nickel, Z. Phys. **33**, 345 (1925).
[30] I. N. Levine, *Quantum Chemistry*, 7th ed. (Pearson, 2013).
[31] Th. Gerrits, M. L. Schneider, A. B. Kos, and T. J. Silva, Large-angle magnetization dynamics measured by time-resolved ferromagnetic resonance, Phys. Rev. B **73**, 094454 (2006).
[32] M. V. Costache, S. M. Watts, M. Sladkov, C. H. van der Wal, and B. J. van Wees, Large cone angle magnetization precession of an individual nanopatterned ferromagnet with dc electrical detection, Appl. Phys. Lett. **89**, 232115 (2006).
[33] N. Kuhlmann, A. Vogel, and G. Meier, Magnetization dynamics and cone angle precession in permalloy rectangles, Phys. Rev. B **85**, 014410 (2012).
[34] N. Mecking, Y. S. Gui, and C.-M. Hu, Microwave photovoltage and photoresistance effects in ferromagnetic microstrips, Phys. Rev. B **76**, 224430 (2007).
[35] R. D. King-Smith and D. Vanderbilt, Theory of polarization of crystalline solids, Phys. Rev. B **47**, 1651 (1993).
[36] D. Vanderbilt and R. D. King-Smith, Electric polarization as a bulk quantity and its relation to surface charge, Phys. Rev. B **48**, 4442 (1993).
[37] R. Resta, Macroscopic polarization in crystalline dielectrics: the geometric phase approach, Rev. Mod. Phys. **66**, 899 (1994).
[38] D. Vanderbilt, *Berry Phases in Electronic Structure Theory: Electric Polarization, Orbital Magnetization and Topological Insulators* (Cambridge University Press, Cambridge, 2018).
[39] See Supplemental Material at http://link.aps.org/supplemental/10.1103/PhysRevB.111.L140409 for the derivation of the orbital pumping coefficients [Eqs. (1) and (2)], proof of the Onsagers reciprocity [Eq. (3)], symmetry constraints on the orbital pumping, and details of first principles calculation, which also includes Refs. [38,40–43,71–76].
[40] A. Crépieux and P. Bruno, Theory of the anomalous Hall effect from the Kubo formula and the Dirac equation, Phys. Rev. B **64**, 014416 (2001).
[41] A. Bastin, C. Lewiner, O. Betbeder-matibet, and P. Nozieres, Quantum oscillations of the Hall effect of a fermion gas with random impurity scattering, J. Phys. Chem. Solids **32**, 1811 (1971).
[42] L Smrcka and P Streda, Transport coefficients in strong magnetic fields, J. Phys. C **10**, 2153 (1977).
[43] R. Kubo, A General expression for the conductivity tensor, Can. J. Phys. **34**, 1274 (1956).
[44] V. Bonbien and Aurélien Manchon, Symmetrized decomposition of the Kubo-Bastin formula, Phys. Rev. B **102**, 085113 (2020).
[45] E. Šimánek and B. Heinrich, Gilbert damping in magnetic multilayers, Phys. Rev. B **67**, 144418 (2003).
[46] D. L. Mills, Ferromagnetic resonance relaxation in ultrathin metal films: The role of the conduction electrons, Phys. Rev. B **68**, 014419 (2003).
[47] B. A. Bernevig, T. L. Hughes, and S.-C. Zhang, Orbitronics: Intrinsic orbital current in p-doped silicon, Phys. Rev. Lett. **95**, 066601 (2005).
[48] H. Kontani, T. Tanaka, D. S. Hirashima, K. Yamada, and J. Inoue, Giant orbital Hall effect in transition metals: Origin of large spin and anomalous Hall effects, Phys. Rev. Lett. **102**, 016601 (2009).
[49] D. Go, D. Jo, C. Kim, and H.-W. Lee, Intrinsic spin and orbital Hall effects from orbital texture, Phys. Rev. Lett. **121**, 086602 (2018).
[50] T. Yoda, T. Yokoyama, and S. Murakami, Orbital Edelstein effect as a condensed-matter analog of solenoids, Nano Lett. **18**, 916 (2018).
[51] L. Salemi, M. Berritta, A. K. Nandy, and P. M. Oppeneer, Orbitally dominated Rashba-Edelstein effect in noncentrosymmetric antiferromagnets, Nat. Commun. **10**, 5381 (2019).
[52] A. Johansson, B. Göbel, J. Henk, M. Bibes, and I. Mertig, Spin and orbital Edelstein effects in a two-dimensional electron gas: Theory and application to $SrTiO_3$ interfaces, Phys. Rev. Res. **3**, 013275 (2021).
[53] F. Freimuth, S. Blügel, and Y. Mokrousov, Spin-orbit torques in Co/Pt(111) and Mn/W(001) magnetic bilayers from first principles, Phys. Rev. B **90**, 174423 (2014).
[54] E. M. Hankiewicz, G. Vignale, and Y. Tserkovnyak, Gilbert damping and spin Coulomb drag in a magnetized electron liquid with spin-orbit interaction, Phys. Rev. B **75**, 174434 (2007).

[55] K. Gilmore, Y. U. Idzerda, and M. D. Stiles, Identification of the dominant precession-damping mechanism in Fe, Co, and Ni by first-principles calculations, Phys. Rev. Lett. **99**, 027204 (2007).

[56] E. Santos, J. E. Abrão, A. S. Vieira, J. B. S. Mendes, R. L. Rodríguez-Suárez, and A. Azevedo, Exploring orbital-charge conversion mediated by interfaces with CuO_x through spin-orbital pumping, Phys. Rev. B **109**, 014420 (2024).

[57] P. Wang, Z. Feng, Y. Yang, D. Zhang, Q. Liu, Z. Xu, Z. Jia, Y. Wu, G. Yu, X. Xu, and Y. Jiang, Inverse orbital Hall effect and orbitronic terahertz emission observed in the materials with weak spin-orbit coupling, npj Quantum Mater. **8**, 28 (2023).

[58] T. S. Seifert, D. Go, H. Hayashi, R. Rouzegar, F. Freimuth, K. Ando, Y. Mokrousov, and T. Kampfrath, Time-domain observation of ballistic orbital-angular-momentum currents with giant relaxation length in tungsten, Nat. Nanotechnol. **18**, 1132 (2023).

[59] Y. Xu, F. Zhang, A. Fert, H.-Y. Jaffres, Y. Liu, R. Xu, Y. Jiang, H. Cheng, and W. Zhao, Orbitronics: light-induced orbital currents in Ni studied by terahertz emission experiments, Nat. Commun. **15**, 2043 (2024).

[60] A. El Hamdi, J.-Y. Chauleau, M. Boselli, Clémentine Thibault, C. Gorini, A. Smogunov, C. Barreteau, S. Gariglio, J.-M. Triscone, and M. Viret, Observation of the orbital inverse Rashba–Edelstein effect, Nat. Phys. **19**, 1855 (2023).

[61] L.-c. Zhang, D. Go, J.-P. Hanke, P. M. Buhl, S. Grytsiuk, S. Blügel, F. R. Lux, and Y. Mokrousov, Imprinting and driving electronic orbital magnetism using magnons, Commun. Phys. **3**, 227 (2020).

[62] L. Alahmed, X. Zhang, J. Wen, Y. Xiong, Y. Li, L.-c. Zhang, F. Lux, F. Freimuth, M. Mahdi, Y. Mokrousov, V. Novosad, W.-K. Kwok, D. Yu, W. Zhang, Y. S. Lee, and P. Li, Evidence of magnon-mediated orbital magnetism in a quasi-2D topological magnon insulator, Nano Lett. **22**, 5114 (2022).

[63] E. Santos, J. E. Abrão, D. Go, L. K. de Assis, Y. Mokrousov, J. B. S. Mendes, and A. Azevedo, Inverse orbital torque via spin-orbital intertwined states, Phys. Rev. Appl. **19**, 014069 (2023).

[64] R. Xu, H. Zhang, Y. Jiang, H. Cheng, Y. Xie, Y. Yao, D. Xiong, Z. Zhu, X. Ning, R. Chen, Y. Huang, S. Xu, J. Cai, Y. Xu, T. Liu, and W. Zhao, Giant orbit-to-charge conversion induced via the inverse orbital Hall effect, arXiv:2308.13144.

[65] S. Mizukami, Y. Ando, and T. Miyazaki, Ferromagnetic resonance linewidth for NM/80NiFe/NM films (NM=Cu, Ta, Pd and Pt), J. Magn. Magn. Mater. **226–230**, 1640 (2001), Proceedings of the International Conference on Magnetism (ICM 2000).

[66] R. Urban, G. Woltersdorf, and B. Heinrich, Gilbert damping in single and multilayer ultrathin films: Role of interfaces in nonlocal spin dynamics, Phys. Rev. Lett. **87**, 217204 (2001).

[67] Y. Liu, Z. Yuan, R. J. H. Wesselink, A. A. Starikov, and P. J. Kelly, Interface enhancement of Gilbert damping from first principles, Phys. Rev. Lett. **113**, 207202 (2014).

[68] X. Ning, A. Pezo, K.-W. Kim, W. Zhao, K.-J. Lee, and A. Manchon, Orbital diffusion, polarization, and swapping in centrosymmetric metals, Phys. Rev. Lett. **134**, 026303 (2025).

[69] S. Han, H.-W. Ko, J. H. Oh, H.-W. Lee, K.-J. Lee, and K.-W. Kim, Orbital pumping incorporating both orbital angular momentum and position, Phys. Rev. Lett. **134**, 036305 (2025).

[70] A. Pezo, D. Go, Y. Mokrousov, H. Jaffrès, and Aurélien Manchon, companion paper, Adiabatic spin and orbital pumping in metallic heterostructures, Phys. Rev. B **111**, 134424 (2025).

[71] D. Wortmann, G. Michalicek, N. Baadji, M. Betzinger, G. Bihlmayer, J. Bröder, T. Burnus, J. Enkovaara, F. Freimuth, C. Friedrich, C.-R. Gerhorst, S. Granberg Cauchi, U. Grytsiuk, A. Hanke, J.-P. Hanke, M. Heide, S. Heinze, R. Hilgers, H. Janssen, D. A. Klüppelberg *et al.*, FLEUR, Zenodo (2024), doi: 10.5281/zenodo.13833162.

[72] E. Wimmer, H. Krakauer, M. Weinert, and A. J. Freeman, Full-potential self-consistent linearized-augmented-plane-wave method for calculating the electronic structure of molecules and surfaces: O_2 molecule, Phys. Rev. B **24**, 864 (1981).

[73] J. P. Perdew, K. Burke, and M. Ernzerhof, Generalized gradient approximation made simple, Phys. Rev. Lett. **77**, 3865 (1996).

[74] F. Freimuth, Y. Mokrousov, D. Wortmann, S. Heinze, and S. Blügel, Maximally localized Wannier functions within the FLAPW formalism, Phys. Rev. B **78**, 035120 (2008).

[75] G. Pizzi, V. Vitale, R. Arita, S. Blügel, F. Freimuth, G. Géranton, M. Gibertini, D. Gresch, C. Johnson, T. Koretsune, J. Ibañez-Azpiroz, H. Lee, J.-M. Lihm, D. Marchand, A. Marrazzo, Y. Mokrousov, J. I. Mustafa, Y. Nohara, Y. Nomura, L. Paulatto *et al.*, Wannier90 as a community code: new features and applications, J. Phys.: Condens. Matter **32**, 165902 (2020).

[76] D. Go, D. Jo, K.-W. Kim, S. Lee, M.-G. Kang, B.-G. Park, S. Blügel, H.-W. Lee, and Y. Mokrousov, Long-range orbital torque by momentum-space hotspots, Phys. Rev. Lett. **130**, 246701 (2023).